ELSEVIER

Journal of Photochemistry and Photobiology A: Chemistry 118 (1998) 71–74

Journal of Photochemistry and Photobiology A:Chemistry

Photodissociation dynamics of formic acid at 193 nm

Seung Keun Shin, Eui Joong Han, Hong Lae Kim*

Department of Chemistry, Kangwon National University, Chuncheon 200-701, South Korea

Received 1 June 1998; received in revised form 31 July 1998; accepted 10 August 1998

Abstract

The photodissociation dynamics of formic acid at 193 nm has been investigated by measuring laser induced fluorescence spectra of OH fragments. From the spectra, fraction of the available energy distributed among the products has been found to be, $f_r(OH) = 0.05$, $f_t = 0.82$, $f_{int}(CHO) = 0.13$, with a negligible fraction of OH being in excited vibrational states. Together with the measured vector correlations, the detailed dynamics of the dissociation process has been discussed. © 1998 Elsevier Science S.A. All rights reserved.

Keywords: Photodissociation dynamics; Formic acid; Vector correlations

1. Introduction

Studies of molecular photodissociation dynamics are of fundamental importance to investigate electronic structures of the molecules because the process is governed by the excited state and potential energy surfaces along the reaction coordinate. The detailed dynamics of the process can be viewed by measuring energies and certain vector properties of the system. These physical properties of the system can precisely be measured from optical spectra in favorable cases where the photofragments absorb and/or emit radiation in an easily accessible spectral region. The Doppler broadened absorption or emission spectra of the photofragments by polarized photolysis and probe light provide information on energy distribution among various degrees of freedom of the fragments as well as directions of the transition dipole moment, recoil velocity and angular momenta of the fragments [1–3]. From the measurements, the excited state and the potential energy surfaces along the reaction coordinate can be identified.

The photodissociation of HCOOH in the first electronic absorption band has long been studied [4–7]. The primary dissociation channels are

$$\begin{aligned} \mathrm{HCOOH} + h\upsilon &\rightarrow \mathrm{HCO} + \mathrm{OH} \\ &\rightarrow \mathrm{COOH} + \mathrm{H} \end{aligned}$$

The measured quantum yield for the OH channel is 0.7∼0.8 [8] while the H atom production channel has recently been identified [9]. In the studies of photodissociation of this molecule mainly at $220 \sim 250$ nm, the very high translational energy of the fragments was measured and almost no vector correlations were observed. It has been concluded that the excited state is predissociative and the dynamics is determined by the late transition state with a dissociation barrier comparable to the available energy of the system [7]. In this case, the dynamics should be similar at higher available energies if the dissociation occurs from the same electronic state. In this study, the detailed photodissociation dynamics of HCOOH at the higher photon energy (193 nm) has been investigated.

The dissociation dynamics has been studied by measuring the laser induced fluorescence spectra of the OH fragments. By analyzing the Doppler profiles of the spectra, the energy distribution and the vector correlations of the fragments have been obtained.

2. Experiment

The experiment has been performed in a flow cell with conventional pump-probe geometry. The cell has been evacuated at a pressure of about 10^{-3} Torr and the gaseous sample has been continuously flowed at a sample pressure of 40 mTorr. The formic acid has been purchased from Aldrich (95% purity) and distilled in vacuum before use.

The 193 nm dissociating light has been obtained from an ArF excimer laser (Lambda Physik Lextra 50), the output of which has been linearly polarized with a stack of quartz plates at a Brewster angle. The horizontally polarized probe light is a frequency-doubled output of a dye laser (Lumonics

*Corresponding author. Tel.: +82-361-50-8480; fax: +82-361-53-7582.

1010-6030/98/$ – see front matter © 1998 Elsevier Science S.A. All rights reserved.
PII: S1010-6030(98)00370-0

HD-500) pumped by the second harmonic of an Nd : YAG laser (Lumonics YM-800). The two laser beams are introduced to the cell at a right angle and are temporally separated by about 50 ns. The 50 ns delay time between the pump and probe lights and 40 mTorr sample pressure should provide a nascent product energy distribution. The laser induced fluorescence (LIF) spectra of the OH fragments have been measured employing the A–X transition in UV. The 0–0 transition of OH has been excited and the resulting total fluorescence has been probed through a cut-off filter at 300 nm. The power of the probe laser light has been kept as low as possible (typically 20 μJ/pulse) to avoid saturation and minimize scattered radiation. The scattered radiation has also been cut off through baffles which are placed in arms attached to the cell. In order to measure the Doppler profiles of the spectra, several rotational transitions have been probed under high resolution. The bandwidth of the probe laser light is 0.07 cm^{-1} in the visible that is measured from the linewidth of the rotationally resolved gaseous I_2 spectra at ambient temperature.

The laser induced fluorescence is detected through a collection lens by a PMT (Hamammatsu R212UH) whose direction of view is at a right angle to the two laser beams, and the detected signal is fed to a boxcar averager. The power of the dissociating and probe light is separately measured and the detected signal is corrected for variation in the laser power. A signal processor digitizes the signal which is stored and processed in a PC.

3. Results and discussion

A portion of the LIF spectra of the OH fragments from HCOOH is presented in Fig. 1. In the spectra, individual rotational transitions in the 0–0 band of the A–X transition are resolved and assigned according to Dieke and Crosswhite [10]. The rotational population distribution is obtained from the measured spectra by using the reported Einstein B coefficients [11]. The distribution is described as a Boltzmann (Fig. 2) with a rotational temperature of 940 K, from which the average rotational energy of OH has been found to be about 660 cm^{-1}. The LIF spectra in the 1–1 band region have been measured but no appreciable intensities have been observed out of noise in the spectra. The diagonal transitions from the higher vibrational states of OH such as 2–2 and 3–3 bands could not be observed due to extensive predissociation from the higher vibrational state in the A state. However, since the measured Doppler lineshape of OH shows no appreciable slow speed components corresponding to the vibrationally excited OH, it has been concluded that the population of OH in the higher vibrational states should be negligible.

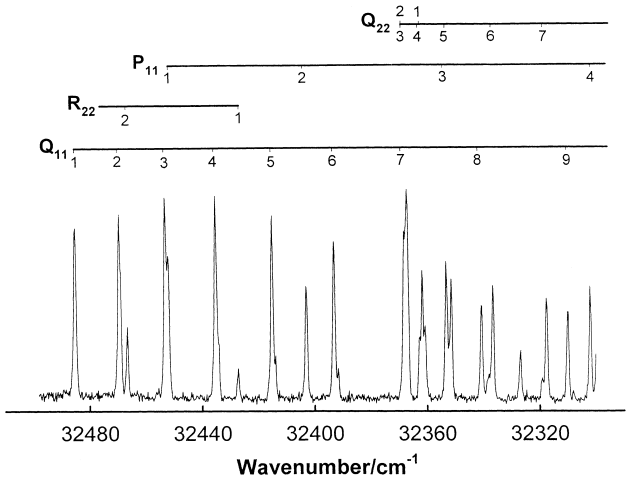

Fig. 1. Portion of the LIF spectra of OH produced from the photodissociation of HCOOH at 193 nm employing the 0–0 band of the A–X transition. Rotational assignments are from Ref. [10].

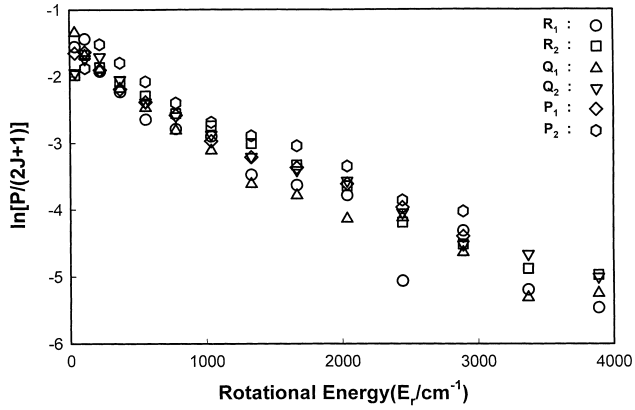

Fig. 2. Boltzmann plot of the observed rotational distribution of OH produced from the photodissociation of HCOOH at 193 nm.

In order to measure translational energies and vector correlations of the OH fragments, the spectra of certain rotational transitions have been measured under higher resolution. In Fig. 3, the measured Doppler profiles are presented for the P and Q branch transitions at the rotational quantum number $N = 6$ with specified experimental geometries. Coupling between translational and rotational motions are thoroughly analyzed by Dixon and Zare [1,2] and the resulting Doppler profiles of the absorption spectra are described by a number of bipolar moments. In the case of photolysis and probe by the linearly polarized lights, the Doppler profiles of the spectra depend upon the excitation–detection geometries, the polarization directions of the lights, and the rotational branch transitions probed. The experimentally measured Doppler profiles are fitted by the equation

$$I(\upsilon) = \int \frac{W(\upsilon)}{2\upsilon}[1 + \beta_{\text{eff}} P_2(\cos\theta_{\varepsilon,z}) P_2(\cos\theta_{v,z})]d\upsilon$$

where P_2 is the second order Legendre polynomials and

$$\beta_{\text{eff}} = \frac{b_2\beta_0^2(20) + b_3\beta_0^0(22) + b_4\beta_0^2(22)}{b_0 + b_1\beta_0^2(02)}$$

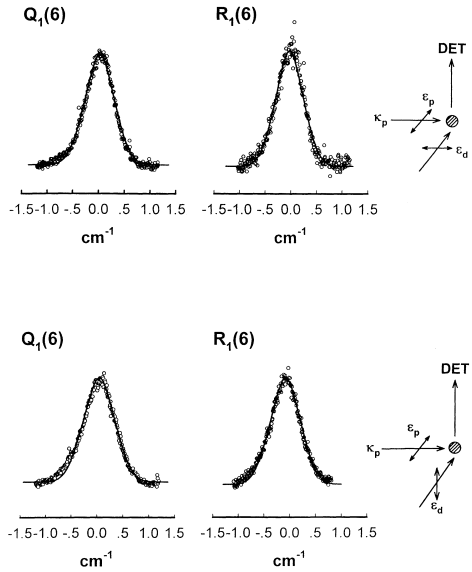

Fig. 3. Doppler profiles of the P- and Q-branch rotational transitions from the rotational state $N = 6$ in the $^2\Pi_{3/2}$ state of OH under two different experimental geometries.

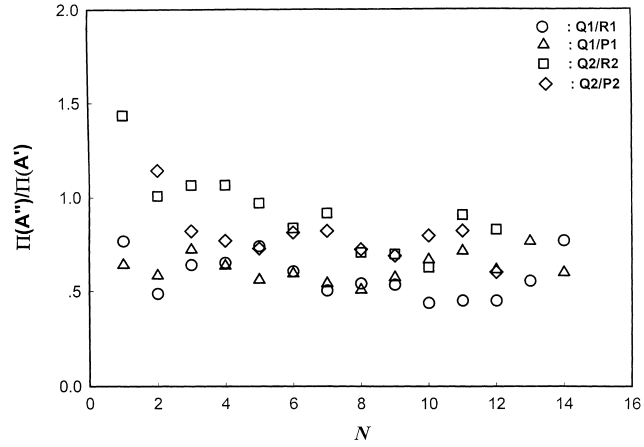

Fig. 4. Λ-doublet distribution of OH obtained from the Q-, P-, and R-branch rotational transitions.

In the above equations, $\beta_0^2(02)$, $\beta_0^2(20)$, $\beta_0^0(22)$, $\beta_0^2(22)$ are the rotational alignment, the translational anisotropy, the v–J correlation, and the (μ–v–J correlation, respectively and bs are obtained from the geometrical parameters and angular momentum coupling factors defined by Dixon [2]. The measured profiles have to be convoluted not only with the laser linewidth but also with a speed distribution which corresponds to internal energies of the sibling fragments, HCO. Since the internal energy of the HCO fragments has not been measured in this experiment, a Gaussian speed distribution with a finite width has been assumed to fit the observed spectra to the above equation. The best fits have been obtained when the average speed of OH is 3200 m/s with the width of 200 m/s. From the average speed, the translational energy of OH has been calculated to be $7290 \pm 470\ \text{cm}^{-1}$ and the center of mass translational energy to be $11{,}560 \pm 750\ \text{cm}^{-1}$.

The observed Doppler profiles for two different rotational branch transitions under two different experimental geometries have made it possible to calculate the four bipolar moments by solving the linear equations. Even though the procedure is approximate, the data satisfactorily provide the quantitative estimates of the vector correlations. The four bipolar moments obtained from the spectra are listed in Table 1. The calculated bipolar moments, that is, the vector correlations are found to be very small. However, the v–J correlation is related to the fraction of the photofragments with $v \| J$ and $v \perp J$, which is given by $f(\|) = 1/3(1 + 2\beta_{vJ})$ and $f(\perp) = 2/3(1\text{-}\beta_{vJ})$, respectively. The measured v–J correlation ($\beta_{vJ} \sim 0$) implies the 70% of the photofragments generated with $v \perp J$, which suggests that OH should rotate in the plane containing the dissociation axis. In Fig. 4, the distribution of OH among the two Λ-doublets is presented. The measured distribution shows a propensity in the A′ state, which suggests that the p_π orbital for the unpaired electron generated upon dissociation lies in the plane of rotation of OH. The rotational motion of the OH fragments originates from the impulsive force upon dissociation producing $v \perp J$ and from the vibrational motions of the parent molecule such as the torsional motion producing $v \| J$. From the measured v–J correlation and the propensity in the A′ state among the two Λ-doublets, it can be concluded that the fragment OH rotation should mainly originate from the impulsive force upon dissociation. In this case, the fraction of the available energy in the OH rotation can be estimated by an impulsive dissociation model.

Table 1
Bipolar moments of the OH fragments produced from the photodissociation of HCOOH at 193 nm

N	$\beta_0^2(02)$	$\beta_0^2(20)$	$\beta_0^2(22)$	$\beta_0^2(22)$
6	0.23	−0.056	−0.00	0.012

The first electronic absorption band of HCOOH in UV starts from 250 nm and peaks around 215 nm but with sharp structures at the long wavelength side [12–14]. The transition is assigned as n(3a″)–π^*(10a′) primarily localized in the C=O moiety and the excited state is predissociative. At 193 nm, the measured absorption cross section is $0.8 \times 10^{-19}\ \text{cm}^2$ compared to the maximum of $1.5 \times 10^{-19}\ \text{cm}^2$ at 215 nm [15]. The next higher energy absorption starts from around 180 nm and peaks at 160 nm [16]. The transition is assigned as π(2a″)–π^*(10a′) and is continuous. Thus at 193 nm, the transition is assumed to be still on the first electronic absorption band. The structured transitions in this band are long progressions of the C=O stretching (υ_3) and the O–C–O bending (υ_7) vibration resulting from structural change from the planar to the pyramidal structure upon absorption due to molecular orbital interactions mentioned by Walsh [17]. Since the transition is vibronically allowed through υ_3 and υ_7, the direction

Table 2
Fraction of the available energy distributed among the products produced from the photodissociation of HCOOH

E_{av} (cm^{-1})[a]	$<f_t>$	$<f_r(OH)>$	$<f_v(OH)>$	$<f_{int}(CHO)>$
At 193 nm				
14,110	0.82	0.05	<0.01[b]	0.13
At 225 nm[c]				
6820	0.78 0.84[d]	0.065	0.03	0.12

[a] $E_{av} = h\upsilon + E_{int}$ (HCOOH at 300 K)$-D_0$ (CHO–OH).
[b] Approximated from the noise in the spectra.
[c] From Ref. [5].
[d] From Ref. [6].

of the transition dipole moment has all three components in space[12]. The measured very small translational anisotropy can be accounted for either by the relatively long predissociative lifetime of the parent molecule or more probably by the spread of the transition dipole moment in space.

Considering the predissociative excited state, the observed energy distributions are surprising. The available energy is the sum of the photon energy (51,730 cm^{-1} at 193 nm) and the internal energy of the parent molecule at room temperature (390 cm^{-1}) minus the dissociation energy ($D_0 = 38{,}010\ cm^{-1}$), which is 14,110 cm^{-1}. The fraction of the measured rotational energy of OH is 0.05 and about 80% of the available energy is found to be transformed into product translation (Table 2). The low vibrational excitation of OH is consistent with the hypothesis that the transition is localized in the C=O moiety and that there is little change in the O–H bond length. The impulsive dissociation model predicts the fraction of the rotational energy of OH is to be 0.03, close to what is observed because the center of mass of OH is located near the O atom. The fraction of the available energy in the rotation of HCO is predicted to be 0.3 from the pyramidal geometry [12,18]. The estimated internal energy of HCO from the experimentally measured translational energy of the products is far less than that predicted by the impulsive model. Thus it suggests the linear O–C–O structure at the transition state by configuration change from the pyramidal excited state.

Upon excitation of the sharp peaks on the long wavelength side of the absorption curve, it has been found that the most of the available energy is transformed into product translation (~80%) and the energy distribution is insensitive to the initial state selection [7]. It has been concluded from the experimental results that the dissociation is predissociative with the late predissociation barrier (>2500 cm^{-1}). The barrier height depends upon the available energies such that the exit channel barrier is nearly equal to E_{av} similar to the case of photodissociation of H_2CO from the A state [19]. Assuming the dissociation proceeds along the C=O vibrationally adiabatic curves strongly coupled to the reaction coordinate, most of the available energy should be channelled into product translation, although the initial excitation introduces many quanta in the C=O vibration. In that case, the pattern of energy disposal should not be significantly changed by increasing the available energy, otherwise the excess energy should, for example, statistically be distributed among all degrees of freedom of the products. In this experiment, the higher photon energy provides higher available energy in the system and yet the observed energy distribution is very similar to the ones from the dissociation at longer wavelengths. The dissociation of HCOOH in the first absorption band in UV indeed occurs in the late transition state where O–C–O bond is nearly linear with the barrier height comparable to the available energy.

Acknowledgements

This work has been supported by the Korea Science and Engineering Foundation and the Ministry of Education of Korea.

References

[1] R.N. Zare, D.R. Herschbach, Proc. IEEE 51 (1963) 173.
[2] R.N. Dixon, J. Chem. Phys. 85 (1986) 1866.
[3] P.L. Houston, J. Phys. Chem. 91 (1987) 5388.
[4] T. Ebata, A. Fujii, T. Amano, M. Ito, J. Phys. Chem. 91 (1987) 6095.
[5] T. Ebata, T. Amano, M. Ito, J. Chem. Phys. 90 (1989) 112.
[6] M. Brouard, J. O'Mahony, Chem. Phys. Lett. 149 (1988) 45.
[7] M. Brouard, J.P. Simons, J.X. Wang, Faraday Discuss. Chem. Soc. 91 (1991) 63.
[8] D.L. Singleton, G. Paraskevopoulos, R.S. Irwin, J. Phys. Chem. 94 (1990) 695.
[9] R. Quandt, Z. Min, X. Wang, H.L. Kim, R. Bersohn, J. Phys. Chem. (1998) submitted to press.
[10] G.H. Dieke, H.M. Crosswhite, J. Quant. Spectrosc. Radiat. Transfer 2 (1962) 97.
[11] I.L. Chidsey, D.R. Crosley, J. Quant. Spectrosc. Radiat. Transfer 23 (1980) 187.
[12] T.L. Ng, S. Bell, J. Mol. Spectrosc. 50 (1974) 166.
[13] C. Fridh, J. Chem. Soc. Faraday Dis. II 74 (1978) 190.
[14] D. Demoulin, Chem. Phys. 17 (1976) 471.
[15] D.L. Singleton, G. Paraskevopoulos, R.S. Irwin, J. Photochem. 37 (1987) 209.
[16] S. Nagakura, K. Kaya, H. Tsubomura, J. Mol. Spectrosc. 12 (1964) 1.
[17] A.D. Walsh, J. Chem. Soc (London) 1953 (1953) 2306.
[18] G.E. Busch, K.R. Wilson, J. Chem. Phys. 56 (1972) 3626.
[19] D.J. Bamford, S.V. Filseth, M.F. Foltz, J.W. Hepburn, C.B. Moore, J. Chem. Phys. 82 (1985) 3032.